Elastic interaction of hydrogen atoms on graphene: A multiscale approach from first principles to continuum elasticity

Paulo S. Branicio,[1,*] Guglielmo Vastola,[1] Mark H. Jhon,[1] Michael B. Sullivan,[1] Vivek B. Shenoy,[2] and David J. Srolovitz[2,3]
[1]*Institute of High Performance Computing, 1 Fusionopolis Way, 16-16 Connexis, 138632, Singapore*
[2]*Department of Materials Science and Engineering, University of Pennsylvania, Philadelphia, Pennsylvania 19104, USA*
[3]*Department Mechanical Engineering and Applied Mechanics, University of Pennsylvania, Philadelphia, Pennsylvania 19104, USA*
(Received 1 May 2016; revised manuscript received 2 August 2016; published 18 October 2016)

The deformation of graphene due to the chemisorption of hydrogen atoms on its surface and the long-range elastic interaction between hydrogen atoms induced by these deformations are investigated using a multiscale approach based on first principles, empirical interactions, and continuum modeling. Focus is given to the intrinsic low-temperature structure and interactions. Therefore, all calculations are performed at $T = 0$, neglecting possible temperature or thermal fluctuation effects. Results from different methods agree well and consistently describe the local deformation of graphene on multiple length scales reaching 500 Å. The results indicate that the elastic interaction mediated by this deformation is significant and depends on the deformation of the graphene sheet both in and out of plane. Surprisingly, despite the isotropic elasticity of graphene, within the linear elastic regime, atoms elastically attract or repel each other depending on (i) the specific site they are chemisorbed; (ii) the relative position of the sites; (iii) and if they are on the same or on opposite surface sides. The interaction energy sign and power-law decay calculated from molecular statics agree well with theoretical predictions from linear elasticity theory, considering in-plane or out-of-plane deformations as a superposition or in a coupled nonlinear approach. Deviations on the exact power law between molecular statics and the linear elastic analysis are evidence of the importance of nonlinear effects on the elasticity of monolayer graphene. These results have implications for the understanding of the generation of clusters and regular formations of hydrogen and other chemisorbed atoms on graphene.

DOI: 10.1103/PhysRevB.94.165420

I. INTRODUCTION

The functionalization of graphene and carbon nanotubes by chemisorption of atoms has tremendous potential for the manipulation of structure and properties [1]. For example, adatoms can modify the electronic properties of graphene, open a band gap, induce magnetic moments, and enhance spin-orbit coupling [2]. Hydrogen chemisorption on graphene also opens new opportunities for hydrogen storage technologies [3–6]. While adsorption of single H on atoms on graphene is well understood, the interactions between such chemisorbed adatoms have received relatively little attention [7]. Nonetheless, these interactions between adatoms determine the ordering and clustering of H atoms on the surface of graphene affecting significantly its properties.

Earlier studies focused upon approaches appropriate for highlighting specific types of interactions. For example, Volpe and Cleri [8] employed a tight-binding model of H to study single H and H pairs on graphene and carbon nanotube surfaces. Yazyev and Helm [9] employed density functional theory (DFT) methods to show how single H "defects" on graphene lead to itinerant magnetism and discussed the magnetic interactions between such H "defects." The induced magnetism was found to be either ferromagnetic or antiferromagnetic depending on whether the H atoms occupy sites on the same or different graphene sublattices. Boukhvalov *et al.* [10] also applied DFT methods to investigate small graphene systems with single or pairs of hydrogen atoms and showed that three-dimensional relaxation of the lattice influences H-H interaction energies. Gargiulo *et al.* [11] in fact demonstrated that the deformations in the graphene sheet generated attractive interactions between hydrogen adatoms that significantly modified their surface arrangement, virtually eliminating isolated hydrogens at room temperature. The importance of the interaction between surface adatoms was emphasized many years ago by Stoneham [7] when he estimated the relative contribution of the long-range elastic interactions between surface adatoms. Such interactions are mediated by the substrate, i.e., one adatom distorts the substrate and the second "feels" that distortion. These interactions are key to explain phenomena such as ordered surface structures and correlated motion of adatom clusters. Peyla *et al.* [12,13] highlighted that the nature of the elastic interactions between defects or adatoms on two-dimensional thin-film surfaces depend on the type of distortion induced by the adatom adsorption. Chen *et al.* [14] employed scanning tunneling microscopy (STM) and DFT to show that the interaction energy between bismuth adatoms on graphene decay as slow as $\sim 1/r$ to $\sim 1/r^2$. Incze *et al.* [15] employed DFT and continuum calculations to show that the interaction between oxygen adatoms on graphene can be either attractive or repulsive depending on the adsorption sites. Shytov *et al.* [16] investigated the electron-mediated long-range interaction between hydrogen adatoms on graphene, assuming that the graphene remained flat. This electronic effect showed attraction between hydrogens on different sublattices and repulsion between H adatoms on the same sublattices, and that these interactions decay slowly, as $1/r$.

The importance of the interaction of adatoms on graphene with topological defects (deformation) was highlighted in a recent study by Cretu *et al.* [17]. They showed experimentally

*braniciol@ihpc.a-star.edu.sg

and through DFT calculations that the interaction between tungsten adatoms and topological defects is strong and influences the surface dynamics of such physisorbed adatoms. Meyer *et al.* [18] used transmission electron microscopy (TEM) to image individual carbon and hydrogen atoms on a graphene surface and showed the formation of small H-atom clusters on graphene. Balog *et al.* [19] further investigated the interaction between hydrogen adatoms and between hydrogen adatoms and surface deformations using STM and came to similar conclusions. They demonstrated that at low H dosage, H adatoms tend to adsorb to convex (protruding) sections of graphene on SiC surfaces. This demonstrates the importance of the elastic deformation of graphene on adatom-adatom and adatom-defect interactions.

The effect of graphene deformation on the chemisorption of hydrogens atoms can also have unexpected implications, as highlighted by Zhang *et al.* [20]. Using atomistic simulations with the empirical REBO2 potential [21] and atomic-level finite-element methods to investigate the bending of graphene nanoribbons (GNR) under chemisorbed and physisorbed hydrogens on graphene, they showed that the sign of the curvature of the GNR surface can be reversed depending on the H dose.

In this study, we employ electronic structure calculations, molecular statics, and continuum methods to study the influence of graphene deformation on hydrogen chemisorption and the long-range elastic interaction between hydrogen atoms, mediated by these deformations. This multiscale approach allows us to describe the deformation on graphene with subangstrom accuracy, and investigate hydrogen interactions from few angstroms to several nanometers. We focus on the description of the intrinsic low-temperature behavior of graphene. Hence, all calculations are performed at $T = 0$, neglecting any temperature or thermal fluctuation effects. We find that the interactions between H-atom pairs depend on the sublattices they are chemisorbed, the orientation of the sites, and the side (i.e., above or below) of the graphene sheet upon which the H atoms reside. The agreement between the different methods validates the predictions and provides a measure of confidence in the accuracy of the predictions.

II. METHODOLOGY

First-principles calculations provide an accurate approach for determining the local bonding of chemisorbed H atoms on graphene surfaces, including both the effects of chemical environment and large local deformation. However, since the system sizes manageable within density functional theory (DFT) approaches are relatively small, such an approach is inappropriate for evaluating the long-range elastic interaction between defects on graphene. We therefore augment such calculations with atomistic molecular statics (MS) and finite-element method (FEM) calculations. It is the comparison between the different methods in the range of mutual validity that provides confidence in the large-scale results. Further, the atomistic methods provide a means of determining the effects of chemical bonding on the deformation that can be used directly in parametrizing the continuum elastic methods.

Density functional theory (DFT) calculations [22,23] were performed within the plane wave and pseudopotential implementation in the QUANTUM ESPRESSO (QE) package [24]. Ultrasoft pseudopotentials[1] were used together with the generalized gradient approximation for the exchange-correlation energy (GGA-PBE) [25]. A 40-Ry cutoff energy was employed and the augmented charge density energy cutoff was set at 400 Ry. Because of the large cell size employed (42.62 Å × 39.36 Å × 15 Å 640 carbon atoms) gamma point sampling yielded sufficient accuracy.

Molecular statics was used to relax large (up to 500 Å × 500 Å) graphene sheets with chemisorbed hydrogens by minimizing the total energy with respect to all atom coordinates using the second-generation reactive empirical bond order potential (REBO2) [21]. Two types of boundary conditions were employed: periodic boundary conditions (for comparison with the DFT results) and free surfaces with clamped (zero out-of-plane displacement) edges for large systems (for comparison with the FEM results).

FEM calculations using the commercial software ABAQUS were used to model the mechanics of membrane deformation induced by chemisorbed H atoms. The graphene sheet was modeled as a thin plate with isotropic elastic constants (Young's modulus $E = 1$ TPa, Poisson's ratio $\nu = 0.25$) [26]. The thickness of the plate was set to $h = 1.35$ Å, such that the bending stiffness of the plate equals that of graphene, as computed with the REBO2 potential [27]. The number density of mesh nodes was chosen to be twice that of graphene lattice sites to ensure sufficient accuracy. The chemisorption of H on graphene was modeled by choosing one mesh node as the FEM-equivalent attachment site of the H atom and defining a surrounding "core" region which accounts for the chemical bonding changes in the vicinity of the H-chemisorption site where sp^2 to sp^3 bonding changes occur. Within the core region (see the schematic in Fig. 1), the formation of each sp^3 bond was modeled with a set of uniaxial and torsional springs. In particular, each spring was modeled using SPRING elements connecting the H-attachment node to each of its attachment nodes. As a result, each bond was represented by two SPRING elements, with one axial spring and one torsional spring. While the axial springs account for the change in bond length, the torsional springs account for the change in the equilibrium angle from the planar sp^2 to the tetrahedrical sp^3 configuration, with an equilibrium bond angle of 109.5°. Two free parameters were required within this model, namely, the equilibrium length of the springs l_e and the Young's modulus of the core region E_c. The numerical value of these parameters was found by ensuring that the springs, in sp^2 configuration, exert to the C atoms the same axial and torsional forces as computed by the atomistic calculations. The numerical estimate for l_e and E_c was $l_e = 3.18$ Å and $E_c = 30$ GPa. The axial and torsional spring constants were $K_a = 9.642$ nN/Å and $K_t = 5.272$ nN/Å, respectively. The large-deformation nature of the displacements (compared to the plate thickness) was accounted for by explicitly activating geometrical nonlinearities in the ABAQUS analysis using the "NLGEOM" keyword.

[1]We used C.pbe-rrkjus.UPF and H.pbe-rrkjus.UPF pseudopotentials for C and H, respectively.

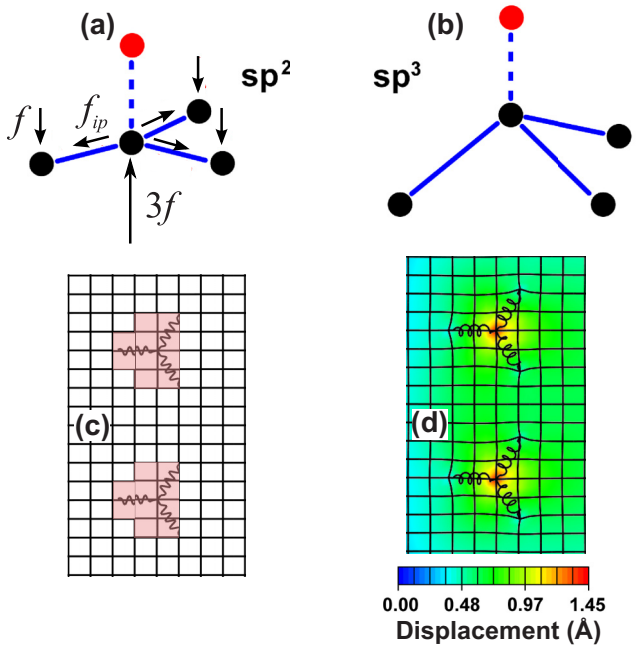

FIG. 1. Schematic representation of the modeling of H chemisorption on graphene using the finite-element method (FEM). (a), (b) Set of springs implemented in the FEM to account for the transition from sp^2 (a) to sp^3 (b) bonding configuration upon the chemisorption of H. Each bond is modeled as a set of axial and a torsional springs acting together. See text for details. (c) Model of two H atoms chemisorbed on graphene in the zigzag direction (relative to each other). The graphene sheet is modeled as a thin plate, with a mesh of node spacing half the atomic nearest-neighbor spacing in the graphene lattice. The shaded area in (c) indicates the elements with modified Young's modulus. (d) Equilibrium configuration as computed by the FEM solver, with colors showing the magnitude of the out-of-plane displacements in angstroms.

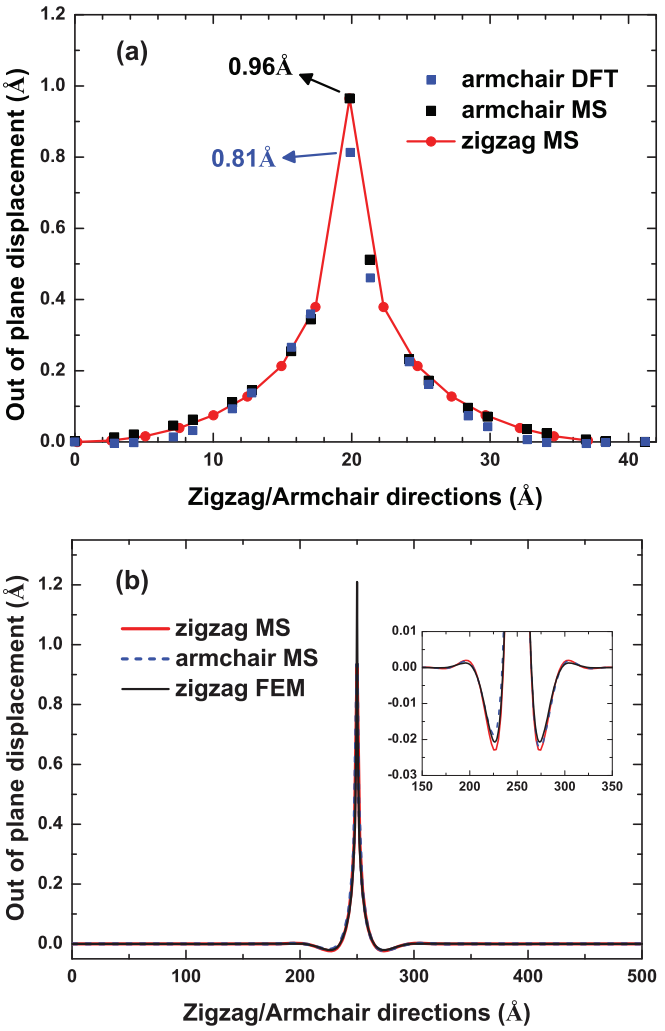

FIG. 2. Out-of-plane displacements of graphene, on chemisorption of a single hydrogen atom, along the zigzag and armchair directions. (a) Density functional theory (DFT) and molecular statics (MS) results for a small rectangular periodic system of ∼40 Å total length along both zigzag and armchair directions. (b) MS and FEM results for a much larger rectangular system with total lengths of ∼Å (periodic boundary conditions are not employed). The inset in (b) shows a zoom-out of the out-of-plane deformation around the chemisorbed H.

III. RESULTS

The deformation profile resulting from the H chemisorption on graphene is the most fundamental data for the determination of the elastic interaction between adatoms on graphene. As highlighted in the Introduction, the interaction between adatoms (as mediated by the graphene deformation) directly influences how adatoms move/adsorb as well as their relative equilibrium position on graphene. We use the molecular statics calculations to determine the stable deformation of graphene upon the chemisorption of hydrogen atoms for several graphene sheet (linear) sizes ranging from a few angstroms up to 500 Å. Because of the importance of this deformation profile, we verify the atomistic results via comparison with the deformation profiles predicted by the DFT calculations for small systems.

The predicted deformation profiles along the armchair and zigzag directions for a rectangular graphene sheet of lateral size ∼40 Å calculated with MS is compared to the predicted deformation profile calculated with DFT in Fig. 2(a). This system contains 641 atoms in both the GGA-PBE DFT and MS calculations. The MS and DFT results agree well and predict a maximum out-of-plane deformation of the hydrogenated carbon of 0.96 Å (MS) and 0.81 Å (DFT), a 19% error. More importantly, the deviation of the MS and DFT results decrease with distance and the overall shape of the deformation profiles are in excellent agreement.

It is interesting to note that the deformation along the armchair and zigzag directions is indistinguishable within the precision of the MS calculations [cf. the MS results in Fig. 2(a)]. This is consistent with the fact that the graphene lattice is elastically isotropic (i.e., it is a honeycomb lattice) and the deformation is consistent with the symmetry of this lattice (i.e., a chemisorbed H atom sits directly over a C atom). We note that a chemisorbed O atom does not sit directly over a C atom in the graphene lattice [15] and, therefore, the displacement fields in the zigzag and armchair directions are expected to be significantly different.

The actual displacement field associated with the chemisorbed H is influenced, to some extent, by the choice of boundary conditions (periodic boundaries are used here) in the small systems such as that shown in Fig. 2. The influence of the boundary conditions is less significant on large graphene sheets. Since DFT calculations are limited to relatively small system sizes, in the remainder of the paper we focus on much larger systems and hence on MS and FEM results.

In order to compare the MS and FEM results, we must first determine the two free parameters that define the FEM model for the local forces associated with H chemisorption. The numerical value of these parameters was found by fitting the axial and torsional forces on the four C atoms nearest the H adsorption site in a flat graphene sheet (using the REBO2 potential). In the sp^2 configuration, the calculated atomistic forces are $f = 2.71$ nN and $f_{ip} = 11.13$ nN [see Fig 1(a)]. The axial and torsional spring constants were $K_a = 9.642$ nN/Å and $K_t = 5.272$ nN/Å.

The MS simulations results for a much larger graphene sheet (~500 Å × 500 Å) with a single chemisorbed H atom is shown in Fig. 2(b) together with the predictions of the continuum elastic FEM calculation. The FEM and MS predictions for the displacements are in excellent agreement across the entire displacement profile, thus validating the FEM approach near the H chemisorption site and the MS simulation results in the far field. As noted above in relation to Fig 2(a), the deformation profile along the zigzag and armchair directions is identical (again, this is as expected since graphene is elastically isotropic within the linear approximation and the local deformation field has the symmetry of the graphene lattice).

Given the deformation profiles (and their validation via a comparison of three different approaches), we now focus on the interaction between chemisorbed hydrogen atoms. The chemisorbed H-H interaction energy was determined by inserting two hydrogens at (above or below) predetermined carbon sites in the graphene lattice and calculating the change in energy:

$$\begin{aligned} U_{\text{H-H}}(r) &= U_{\text{G+2H}}(r) - U_{\text{G}} - 2U_{\text{H}} \\ &\quad -2(U_{\text{G+1H}} - U_{\text{G}} - U_{\text{H}}) \\ &= U_{\text{G+2H}}(r) - 2U_{\text{G+1H}} + U_{\text{G}}, \end{aligned} \tag{1}$$

where $U_{\text{G+2H}}(r)$ is the total energy of the system with two hydrogens separated by a distance r, U_{G} is the energy of the graphene system with no hydrogen, U_{H} is the energy of an isolated hydrogen atom, and $U_{\text{G+1H}}$ the total energy of the system with a single chemisorbed hydrogen.

In looking at chemisorbed H-H interactions, it is useful to distinguish between the orientations of the vectors separating the H atoms, the sublattices of the C atoms to which the H atoms are chemisorbed, and whether the H atom is chemisorbed above or below the graphene sheet. The honeycomb lattice [see Fig. 3(a)] is composed of two distinct triangular sublattices [shown as yellow or white C atoms in Fig. 3(a) and referred to as the *A* or *B* sublattices, respectively]. H atoms can be chemically bonded to the same C atom either above or below the graphene sheet, which we refer to as + or −. Finally, a pair of chemisorbed H atoms can be oriented relative to one another along different directions (relative to the graphene structure), which we label by the angle θ ($\theta = n\pi/3$ for the armchair direction and $\theta = n\pi/3 - \pi/6$ for the zigzag direction, where $n = 0$, 1, or 2). Figure 3(b) shows a pair of chemisorbed H atoms along the zigzag direction. All of the atoms along a vector drawn in the zigzag direction are on the same sublattice. On the other hand, as shown in Figs. 3(c) and 3(d), along the armchair direction the C atoms to which the hydrogens are chemisorbed can be either on the *A* or *B* sublattice. These two armchair cases are inequivalent. Further, the armchair configurations are not symmetric with respect to rotations by π. The equivalent directions are $2\pi/3$ apart (the $\theta = 0$, $2\pi/3$, and $4\pi/3$ are equivalent, as are those at $\theta = \pi/3$, π, and $5\pi/3$).

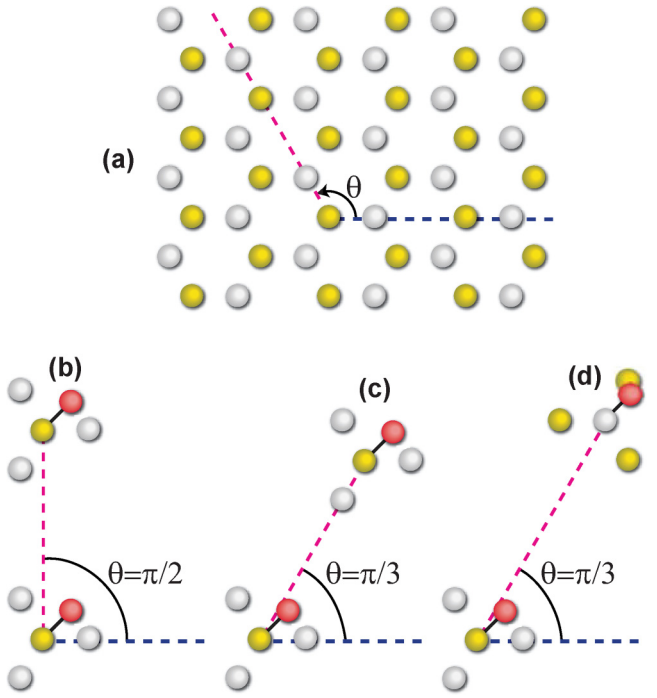

FIG. 3. The graphene lattice and the location of chemisorbed H pairs. (a) The honeycomb graphene lattice showing the *A* (yellow carbon atoms) and *B* (white carbon atoms) triangular sublattices. (b) Pairs of H atoms (shown in red) chemisorbed to C atoms along the zigzag direction $\theta = \pi/2$. (c) Pairs of H atoms chemisorbed to C atoms on the *same* sublattice (both yellow/*A* here) along the armchair direction $\theta = \pi/3$. (d) Pairs of H atoms chemisorbed to C atoms on *different* sublattices (yellow/*A* and white/*B*) along the armchair direction $\theta = \pi/3$.

Figure 4(a) shows the interaction energy between a pair of chemisorbed H atoms along the zigzag direction on the same side of the graphene sheet (+/+ or −/−). These H atoms repel one another at all separations. On the other hand, H atoms chemisorbed on opposite sides of the graphene sheet (+/−), attract one another at all separations [see Fig. 4(b)] except the smallest separation. The repulsive interaction at that distance can be attributed to direct chemical interactions between the H atoms (i.e., the H atoms change the bond order of the carbon atoms that are nearest neighbors to the C atom to which it is chemisorbed). All data used to plot Figs. 2 and 4 are provided as Supplemental Material [28].

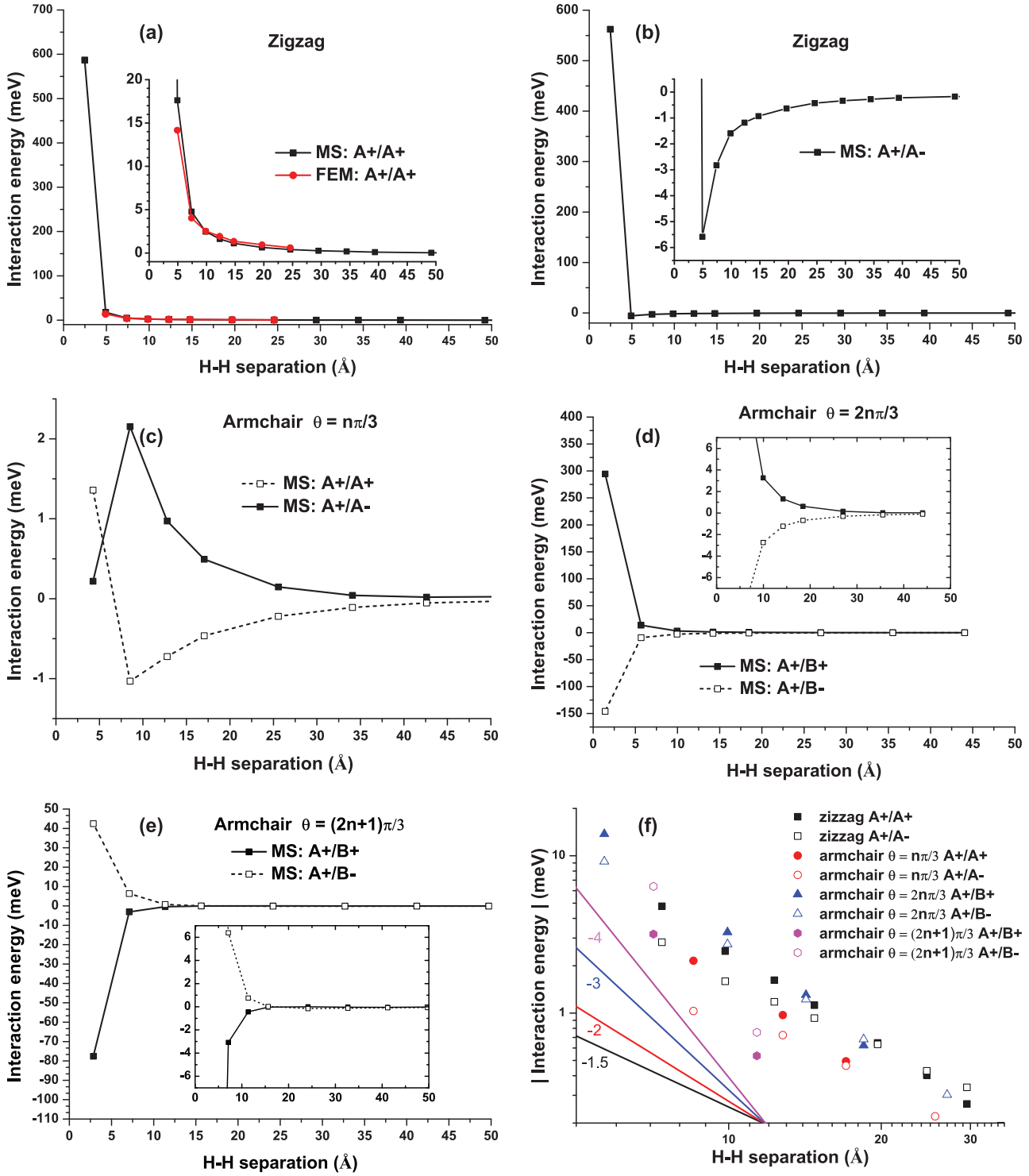

FIG. 4. Interaction energies along the zigzag and armchair directions as a function of the separation between hydrogen and the chemisorption side. Hydrogens along the zigzag direction on the same (a) and opposite (b) graphene sides. Results are shown for both MS and FEM. Hydrogens along the armchair on the same and opposite sides on the same sublattice (c); and different sublattices with $\theta = 0$ (d) and $\theta = \pi$ (e), following the schematics defined in Fig. 3. (f) Comparison of elastic interactions along different directions with power-law decays. The dashed lines of different slopes are drawn as guides to the eye only.

Figures 4(a) and 4(b) show the interaction energy between chemisorbed H atoms as determined using the FEM approach. The consistency of the FEM and MS results demonstrates that the interaction between chemisorbed H atoms is dominated by elastic effects beyond just a couple of interatomic distances.

We next turn to the H interactions along the armchair direction [Figs. 3(c) and 3(d)]. Unlike in the zigzag direction case, the elastic interactions along the armchair direction show different trends if the pair of H atoms are on the same sublattice or on different sublattices. For the case where both H atoms are

on the same sublattice, A/A [as shown in Figs. 4(c) and 3(a)], the H-H interaction energies are very small compared with those along the zigzag direction. The error in determining the interaction energies is $\leqslant 1$ meV. Comparing the cases where the hydrogens are on the same ($A+/A+$) or different ($A+/A-$) sides of the graphene sheet [Fig. 4(c)], we find that the signs of the interaction energies are reversed: repulsive for $A+/A+$ and attractive for $A+/A-$. This implies that it is energetically favorable for H chemisorption to occur on both sides of the graphene sheet along the armchair direction on the same sublattice.

As discussed above, there is an armchair direction every $\pi/3$ in the graphene lattice, but that the symmetry associated with pairs of carbon atoms along $\theta = n2\pi/3$ is inequivalent to those at $\theta = \pi/3(2n+1)$ for $n = 0$, 1, or 2. Figures 4(d) and 4(e) show the interaction energy results for the $\theta = n2\pi/3$ and $\pi/3(2n+1)$ cases, respectively. The results are remarkably similar, except for one profound difference. That is, the interactions have opposite signs.

IV. DISCUSSION

Our use of the REBO potential naturally restricts the interactions studied in this paper to be mechanical in nature. We note that there are other proposed interactions that are electron mediated (such as that proposed by Shytov *et al.* [16], Chen *et al.* [14], and Lin *et al.* [29]). However, our present study does not explicitly include these mechanisms: as a result, we analyze only the mechanical component of the MS interaction energies. We note that the interaction energy between nearest neighbors can be very different (in sign and magnitude) from the long-range mechanical interaction. As described earlier, in the continuum analysis we model chemisorbed hydrogen as a set of point forces on an elastic plate. In the limit of linear deformation, the out-of-plane displacements w become decoupled from the in-plane stretching. In this limit, w must satisfy the biharmonic equation $\nabla^2\nabla^2 w = 0$ and the in-plane displacements must satisfy the Lamé equations [30].

To calculate the interaction energy due to out-of-plane deformation, we recall the elementary solution [30] to an isolated point force applied normal to a clamped plate of radius R:

$$w(r) = \frac{3f(1-\nu^2)}{2\pi Eh^3}. \tag{2}$$

Assuming that the radius of the plate is much larger than the interatomic spacing, we can construct the out-of-plane deformation (to leading order) for a single H atom using superposition. The leading-order term is radially isotropic and can be written as

$$w(r) = \frac{3a^2 f(1-\nu^2)[1+2r-2r\ln(R/r)]}{4h^3\pi r E}, \tag{3}$$

where a is the bond length between carbon atoms, and the rest of the variables are as defined previously. Equation (3) does not reflect all of the features that we observed in our atomistic simulations. In particular, it decreases monotonically away from the adsorbed H atom, and does not replicate the local minima observed in Fig. 2(b). Nonetheless, if this is the leading-order term in the displacement, it is possible to estimate the interaction energy from the expression [15]

$$E_{el} = -\frac{1}{2}\left[\sum_{i=1}^{N} f_i^{(\alpha)} w^{(\beta)}(\mathbf{a}_i) + \sum_{j=1}^{N} f_j^{(\beta)} w^{(\alpha)}(\mathbf{R}+\mathbf{b}_i)\right], \tag{4}$$

where we have considered only out-of-plane displacements. α and β are labels for the two hydrogens and the force distributions are described by the groups of vectors $\mathbf{a}_i$ and $\mathbf{b}_j$.

By using the force distribution consistent with the chemisorbed hydrogens, we can find expressions for the interaction energy if the adsorbed H atoms are on the same sublattice

$$E^s_{\text{bend}} = \mp\frac{(1-\nu^2)f^2a^6}{\pi Eh^3r^4}\cos(6\theta) \tag{5}$$

or on different sublattices,

$$E^s_{\text{bend}} = \pm\frac{(1-\nu^2)f^2a^5}{2\pi Eh^3r^3}\cos(3\theta). \tag{6}$$

The $\mp$ ($\pm$) in these expressions refers to the sign of the interaction when the hydrogens are on the same (different) sides. These expressions are consistent with a more general theory developed by Marchenko and Misbah [31]. Examination of Eqs. (5) and (6) shows that the interaction energies decay as $1/r^4$ (same sublattice) or $1/r^3$ (different sublattices).

The power law of the radial decay is a key feature of the interaction energy. It indicates the length scale for which these interactions are important. Up until this point, we have ignored contributions to the interaction energy from stretching in the plane. An analysis of point defects interacting only via in-plane displacements was performed by Peyla *et al.* [12,13]. They likewise found that the interaction energy depends on whether or not the defects lie on the same sublattice. We can apply their theory to H adsorption on graphene. If two H atoms chemisorb onto the same sublattice, the leading-order term in the interaction energy is

$$E^s_{\text{stretch}} = -27\frac{(1+\nu)^2 f_{ip}^2 a^4}{4\pi Ehr^4}\cos(6\theta). \tag{7}$$

If the two H atoms are on different sublattices, then the interaction energy is, to leading order,

$$E^o_{\text{stretch}} = 9\frac{(1+\nu)^2 f_{ip}^2 a^3}{8\pi Ehr^3}\cos(3\theta). \tag{8}$$

This stretching analysis considers nominally flat graphene, and does not account for whether the H is chemisorbed above or below the graphene sheet. The interaction energy due to stretching is likely very small: the in-plane stretching will be relaxed by local buckling of the sp^3 hybridized C atom out of the graphene plane. However, it is worth noting that for this geometry, the power laws are identical for stretching and bending. Even if stretching energy is dominant in the linear limit, it should not change the observed power-law decay for H-H interactions.

We compare our predicted power laws to those calculated from MS in Table I. We find that the linear theory approach is sufficient to determine the sign of all the interactions. The

TABLE I. Exponents from least-squares fit of interactions to power law of the form Ax^{-m}. Note that that only data for spacings between 5 and 50 Å were used in the fit.

			MS			Theory	
Direction	Case	Angle	Sign	m	R^2	Sign	m
Zigzag	$A+/A+$	$n\pi/2$	+	2.4	0.977	+	4
Zigzag	$A+/A-$	$n\pi/2$	−	1.5	0.996	−	4
Armchair	$A+/A+$	$n\pi/3$	−	3.0	0.98	−	4
Armchair	$A+/A-$	$n\pi/3$	+	2.3	0.91	+	4
Armchair	$A+/B+$	$2n\pi/3$	+	3.4	0.97	+	3
Armchair	$A+/B-$	$2n\pi/3$	−	2.2	0.91	−	3
Armchair	$A+/B+$	$(2n+1)\pi/3$	−	3.0	0.75	−	3
Armchair	$A+/B-$	$(2n+1)\pi/3$	+			+	3

analysis is also able to qualitatively explain the dependence of the interaction energy on the local symmetry of the adsorbate. It distinguishes between the sign of interactions when the H atoms have chemisorbed on the same and different sides of the graphene as well as on the same or different sublattices. This interaction has an angular dependence that accounts for the observed anisotropy in the zigzag and armchair directions.

In contrast, Table I shows that the power law for interactions between adsorbed H atoms on the same and different sublattices from MS calculations, 1.5–3.0, are lower than those predicted from the linear elasticity theory, 3–4. The differences between the predicted and calculated power laws may be related to a failure of the linear approximation assumed in the predictions. The geometric nonlinearity of the graphene sheet deformation may induce important coupling between in-plane and out-of-plane deformations that are not included in the current linear approach. In fact, such an approach considering the nonlinear deformation of a thin film in the general case when tangential and normal forces are combined was taken recently by He [32]. He considered twofold and threefold force distributions in the analysis. The latter can be applied to our case of H adsorption in graphene. The predictions show that the power law $1/r^4$ is only valid in the particular case of same sublattices aligned at $n\pi/2$ as shown in the first two entries of Table I. In all other cases, the nonlinear approach predicts a power law $1/r^3$.

While the honeycomb of graphene corresponds to an isotropic fourth-order elastic tensor (linear elasticity), previous investigations have in fact shown that within a nonlinear approach the six-order elastic tensor is anisotropic [33–38]. Therefore, considering the fundamental differences between the MS and elasticity approaches, it is somehow surprising that the latter is fully able to explain the essential features of the H-H elastic interaction. The general agreement in sign of interactions and power laws is also noticeably good. Other differences in approach include system size; i.e., due to computational constraints in the MS calculations a finite system with clamped edges is used, while in the elasticity approach a film extending infinitely in the plane is considered. In addition, the elasticity approach assumes an isolated force normal to a clamped plate, while in the MS approach the many-body force induced by the chemisorption of an H atom results in significant chemical changes and atomic net forces extending up to the second atomic shell of the C atom hosting the H adatom. Therefore, considering all these differences in approach, the agreement in sign and power law of the interaction is fairly good. One should also note that the accuracy of the interaction energy from MS is not only affected by the size of system. The interaction energy is in the order of meV at long distances and close to the numerical precision limit of our double-precision MS calculation. Increasing the size of system to further relax the deformations and possibly improve the calculation of the power laws results actually in lower accuracy since larger systems further reduce the number of significant digits of the interaction energy calculated from energy differences.

Hence, while we expect that the MS adatom interaction eventually converges to the elasticity predicted power laws for sufficiently large systems, that may never occur for finite graphene with clamped edges. Notwithstanding, the MS results are valuable to understand how adatom clusters are formed. Considering the predictions of strong long-range interactions of this study it is not surprising, for example, that isolated H adatoms on graphene are absent in room temperature experiments, when their surface mobility is considerable [11]. The results also explain the tendency for formation of H dimers and elongated small clusters, as they are energetically favorable configurations [2,11].

We expect the predictions of this work to be valid for other adatoms on graphene as well, if the main effect of the chemisorption is a change in hybridization at the C host atom, e.g., H chemisorption induces a sp^2 to sp^3 hybridization change. Otherwise, a threefold symmetric deformation induced by the adsorption of an adatom on top of a C host atom would also induce similar elastic deformations and interactions. Even though all the calculations in this work are performed considering the atomic deformations induced by H chemisorption, such graphene deformations can be induced by adsorption of several other chemical species and molecules. The induced elastic interactions as described by the elasticity theory analysis are oblivious to the differences in adatom chemistry, and the adatom energy interaction sign and power laws would be similar. Nakada and Ishii [39] evaluated the adsorption energies in different adsorption sites on graphene for atomic species covering almost the entire periodic table. From their calculations the following species adsorb preferentially onto C atoms: H, F, Cl, Br, I, Ag, and Au. We thus expect that our calculations would be useful to explain the spatial distribution and formation of adatom clusters on graphene of all these atomic species.

In this study, we have focused on the structure and interactions of graphene at $T = 0$, neglecting thermal fluctuations of the graphene sheet. However, recent studies [40,41] have shown that such thermal fluctuations have important consequences for their mechanical properties. In particular, the finite-temperature in-plane elastic moduli of graphene decreases with system size L following a power-law decay $L^{-0.325}$. Considering our continuum elasticity analysis in light of this result suggests that the interaction between adatoms on graphene may be highly dependent on both temperature and on the size of the graphene sheet. These topics deserve further theoretical and experimental consideration.

V. CONCLUSIONS

We have employed a multiscale approach combining density functional theory, molecular statics, finite-element modeling, and elastic plate theory to investigate the deformation of graphene due to the chemisorption of a single hydrogen atom. We found an isotropic deformation profile due to the adsorption of an isolated H atom on a large graphene sheet with three methods (DFT, MS, and FEM), which are consistent to within subangstrom resolution. We calculated numerically the interaction between chemisorbed H pairs for H-H spacings up to 50 Å. Despite the linear isotropic elasticity of graphene, the interaction of H pairs depends strongly on the local symmetry of carbons onto which the H atoms adsorb. In particular, the sign of the interaction depends on which sublattice and the side of the graphene sheet the H atoms adsorb onto. H pairs along the zigzag direction attract each other if they are on the same side of the sheet and repel each other otherwise. The interaction of the H pairs along the armchair direction depends on their relative angle. Given the differences in approach, elasticity theory predictions and molecular statics calculations agree reasonably well on the sign and power-law decay of the interactions. The difference in power-law decay calculated using molecular statics and those from the elasticity analysis is an indication of the effects of nonlinear elasticity of graphene. The predictions on the interaction between H pairs are able to explain experimental arrangements of H adatoms on graphene and we expect that the results are also useful to explain the arrangement of other adatoms that share the same preferential adsorption site on top of C atoms.

ACKNOWLEDGMENT

The computational part of this work was supported by the A*STAR Computational Resource Centre (A*CRC) through the use of its high performance computing facilities.

[1] J. Balakrishnan, G. Koon, J. Jaiswal, A. C. Neto, and B. Ozyilmaz, Nat. Phys. **9**, 284 (2013).
[2] J. Katoch, Synth. Met. **210**, Part A, 68 (2015).
[3] A. Dillon and M. Heben, Appl. Phys. A **72**, 133 (2001).
[4] J. Zhao, A. Buldum, J. Han, and J. P. Lu, Nanotechnology **13**, 195 (2002).
[5] S. Patchkovskii, J. S. Tse, S. N. Yurchenko, L. Zhechkov, T. Heine, and G. Seifert, Proc. Natl. Acad. Sci. USA **102**, 10439 (2005).
[6] M. Pumera, Energy Environ. Sci. **4**, 668 (2011).
[7] A. M. Stoneham, Solid State Commun. **24**, 425 (1977).
[8] M. Volpe and F. Cleri, Surf. Sci. **544**, 24 (2003).
[9] O. V. Yazyev and L. Helm, Phys. Rev. B **75**, 125408 (2007).
[10] D. W. Boukhvalov, M. I. Katsnelson, and A. I. Lichtenstein, Phys. Rev. B **77**, 035427 (2008).
[11] F. Gargiulo, G. Autès, N. Virk, S. Barthel, M. Rösner, L. R. M. Toller, T. O. Wehling, and O. V. Yazyev, Phys. Rev. Lett. **113**, 246601 (2014).
[12] P. Peyla, A. Vallat, C. Misbah, and H. Muller-Krumbhaar, Phys. Rev. Lett. **82**, 787 (1999).
[13] P. Peyla and C. Misbah, Eur. Phys. J. B **33**, 233 (2003).
[14] H.-H. Chen, S. Su, S.-L. Chang, B.-Y. Cheng, C.-W. Chong, J. Huang, and M.-F. Lin, Carbon **93**, 180 (2015).
[15] A. Incze, A. Pasturel, and P. Peyla, Phys. Rev. B **66**, 172101 (2002).
[16] A. V. Shytov, D. A. Abanin, and L. S. Levitov, Phys. Rev. Lett. **103**, 016806 (2009).
[17] O. Cretu, A. V. Krasheninnikov, J. A. Rodriguez-Manzo, L. T. Sun, R. M. Nieminen, and F. Banhart, Phys. Rev. Lett. **105**, 196102 (2010).
[18] J. C. Meyer, C. O. Girit, M. F. Crommie, and A. Zettl, Nature (London) **454**, 319 (2008).
[19] R. Balog, B. Jrgensen, J. Wells, E. Lgsgaard, P. Hofmann, F. Besenbacher, and L. Hornekr, J. Am. Chem. Soc. **131**, 8744 (2009).
[20] Z. Zhang, B. Liu, K. C. Hwang, and H. Gao, Appl. Phys. Lett. **98**, 121909 (2011).
[21] D. W. Brenner, O. A. Shenderova, J. A. Harrison, S. J. Stuart, B. Ni, and S. B. Sinnott, J. Phys.: Condens. Matter **14**, 783 (2002).
[22] P. Hohenberg and W. Kohn, Phys. Rev. **136**, B864 (1964).
[23] W. Kohn and L. J. Sham, Phys. Rev. **140**, A1133 (1965).
[24] P. Giannozzi, S. Baroni, N. Bonini, M. Calandra, R. Car, C. Cavazzoni, D. Ceresoli, G. L. Chiarotti, M. Cococcioni, I. Dabo, A. Dal Corso, S. Fabris, G. Fratesi, S. de Gironcoli, R. Gebauer, U. Gerstmann, C. Gougoussis, A. Kokalj, M. Lazzeri, L. Martin-Samos, N. Marzari, F. Mauri, R. Mazzarello, S. Paolini, A. Pasquarello, L. Paulatto, C. Sbraccia, S. Scandolo, G. Sclauzero, A. P. Seitsonen, A. Smogunov, P. Umari, and R. M. Wentzcovitch, J. Phys.: Condens. Matter **21**, 395502 (2009).
[25] J. P. Perdew, K. Burke, and M. Ernzerhof, Phys. Rev. Lett. **77**, 3865 (1996).
[26] C. D. Reddy, S. Radjendran, and K. M. Liew, Int. J. Nanosci. **4**, 631 (2005).
[27] V. B. Shenoy, C. D. Reddy, A. Ramasubramaniam, and Y. W. Zhang, Phys. Rev. Lett. **101**, 245501 (2008).
[28] See Supplemental Material at http://link.aps.org/supplemental/10.1103/PhysRevB.94.165420 for data used to plot Figs. 2 and 4.
[29] Y. Lin, F. Ding, and B. I. Yakobson, Phys. Rev. B **78**, 041402 (2008).
[30] L. D. Landau and E. M. Lifshitz, *Theory of Elasticity*, 3rd ed., Theoretical Physics (Butterworth-Heinemann, Oxford, 1986).
[31] V. I. Marchenko and C. Misbah, Eur. Phys. J. E **8**, 477 (2002).
[32] L. H. He, Phys. Rev. E **89**, 062409 (2014).
[33] E. Cadelano, P. L. Palla, S. Giordano, and L. Colombo, Phys. Rev. Lett. **102**, 235502 (2009).
[34] E. Cadelano, S. Giordano, and L. Colombo, Phys. Rev. B **81**, 144105 (2010).

[35] L. Colombo and S. Giordano, Rep. Prog. Phys. **74**, 116501 (2011).
[36] L. Zhou, Y. Wang, and G. Cao, J. Phys.: Condens. Matter **25**, 125302 (2013).
[37] R. Dettori, E. Cadelano, and L. Colombo, J. Phys.: Condens. Matter **24**, 104020 (2012).
[38] L. Zhou and G. Cao, Phys. Chem. Chem. Phys. **18**, 1657 (2016).
[39] K. Nakada and A. Ishii, Solid State Commun. **151**, 13 (2011).
[40] J. H. Los, A. Fasolino, and M. I. Katsnelson, Phys. Rev. Lett. **116**, 015901 (2016).
[41] A. Košmrlj and D. R. Nelson, Phys. Rev. B **93**, 125431 (2016).